Phosphoramidate Prodrugs Continue to Deliver, The Journey of Remdesivir (GS-5734) from RSV to SARS-CoV-2

Richard L. Mackman*

Cite This: *ACS Med. Chem. Lett.* 2022, 13, 338−347

Read Online

ACCESS | Metrics & More | Article Recommendations | SI Supporting Information

ABSTRACT: Remdesivir (GS-5734) is a monophenol, 2-ethyl-butylalanine phosphoramidate prodrug of a 1′-cyano-4-aza-7,9-dideazaadenosine C-nucleoside (GS-441524) that is FDA approved for the treatment of hospitalized patients with COVID-19. The prodrug, initially invented for respiratory syncytial virus, was later found to have activity toward emerging RNA viruses, including Ebola and coronaviruses. Remdesivir is among the first examples of a phosphoramidate prodrug aimed at delivering a nucleoside monophosphate into lung cells to efficiently generate the nucleoside triphosphate inhibitor of viral RNA polymerases. With remdesivir as the central case study, the present work describes the antiviral potency and in vitro metabolism evidence for lung cell activation of phosphoramidates, together with their in vivo pharmacokinetics, lung distribution, and antiviral efficacy toward respiratory viruses. The lung delivery of nucleoside monophosphate analogs using prodrugs warrants further investigation toward the development of novel respiratory antivirals.

KEYWORDS: Remdesivir, Antiviral, Nucleoside, Prodrug, Phosphoramidate, SARS-CoV-2
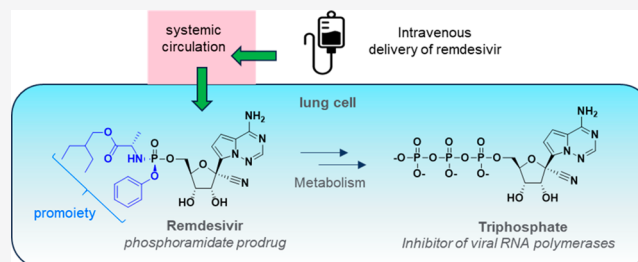
At the heart of all small molecule drug discovery programs lies one basic question with which all teams wrestle: how do I deliver the active drug to the molecular target safely in patients? Identifying superbly potent and selective modulators of a target is often the most straightforward aspect of the drug discovery process, and it is the safe and effective delivery of the active compound to the molecular target within the human body that consumes the most time and resources. It is especially challenging to achieve the desired in vivo distribution of the inhibitor when the target is intracellular and the mechanism of action for the inhibitor mandates chemical matter that has intrinsically poor permeability and access into the target tissue. For example, inhibitors that are predominantly charged and, therefore, highly polar at physiological pH, such as carboxylic acids, phosphates, or highly basic amines. It is in these situations that prodrugs can favorably change the in vivo distribution of a compound potentially transforming a "potent biochemical inhibitor" into a potential "drug".

Remdesivir (**1**, GS-5734, Veklury, Figure 1) is an mono-phenol, 2-ethylbutylalanine phosphoramidate prodrug of a 1′-CN C-nucleoside **2** that was originally invented as a potential treatment for respiratory syncytial virus (RSV), a virus that has high morbidity in vulnerable infants and elderly patients.[1] Following the start of the West Africa Ebola outbreak in 2013, **1** was shown through screening to also exhibit potent inhibition of Ebola virus, and in response to the escalating crisis we elected to advance **1** into clinical studies as a matter of urgency.[2,3] Although the development of **1** as a potential treatment for Ebola was halted following a Phase 2 study, its antiviral activity extended to many other RNA viruses beyond RSV and Ebola, including coronaviruses.[4,5] In early 2020, shortly after the identification of SARS-CoV-2, Gilead initiated clinical studies of **1** for COVID-19 treatment, and in October 2020, **1** became the first small molecule antiviral to be approved by the FDA for the treatment of hospitalized patients with COVID-19.

Aryloxy phosphoramidate prodrugs (from here abbreviated as phosphoramidates) are best known for their application in delivering antiviral nucleoside monophosphate payloads into immune cells and hepatocytes to target HIV and hepatitis C virus (HCV), respectively.[6−8] The prodrug design includes an aryloxy group and an amino acid ester group, that together mask the ionizable groups of the monophosphate nucleotide (Figure 1). Once the promoieties are cleaved inside cells, the monophosphate, for example, **1**-MP, is released, which can then be anabolized by intracellular phosphorylating enzymes into the biologically active triphosphate (TP) inhibitor of viral replication, for example, **1**-TP. The original phosphoramidate prodrug design of **1** is noteworthy because the targeted monophosphate prodrug on parent **2** was found to substantially increase the levels of **1**-TP formed in primary lung cells in vitro
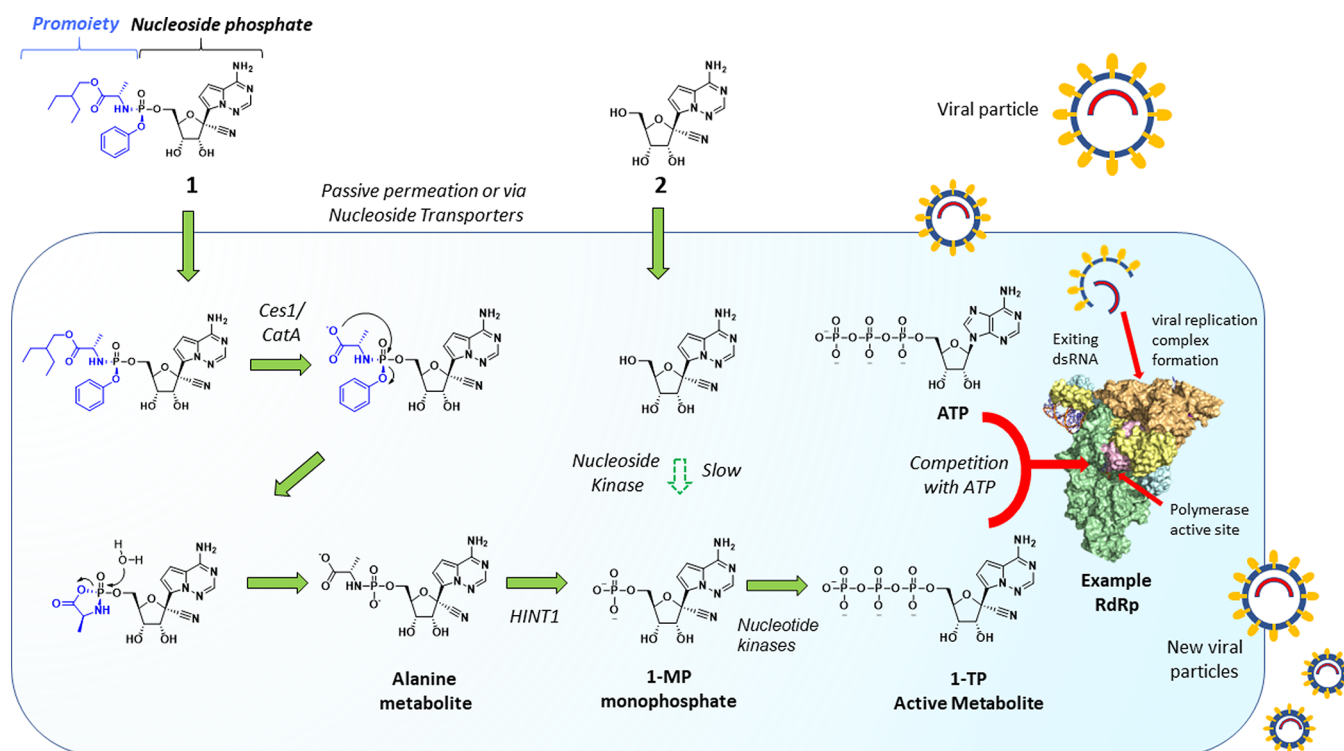
Figure 1. Proposed cellular activation pathway of prodrug **1** and parent nucleoside **2** leading to the formation of **1**-TP and inhibition of a representative RNA-dependent RNA polymerase (RdRp). Following passive or transporter-mediated entry into the cell, the promoiety (blue) in **1** is metabolized by host enzymes to release **1**-MP; while in many cells, nucleoside **2** is often significantly slower to anabolize to **1**-MP by the action of a cellular kinase. **1**-MP is converted to **1**-TP by cellular kinases and competes with ATP for incorporation into viral RNA to inhibit replication.

leading to improved RSV potency.[1] Importantly, in vivo experiments subsequently established that the prodrug **1** is also capable of delivering **1**-TP into the lungs of animals more efficiently than the parent nucleoside **2** leading to anti-RSV activity in vivo. To the best of our knowledge, at the time **1** was invented, there was no published in vitro or in vivo evidence attempting to employ the phosphoramidate prodrug approach to effectively deliver a monophosphate nucleoside analog into lung cells for inhibition of a respiratory virus. The invention of **1** and its ability to generate active **1**-TP in lungs supports the potential that this approach might be more broadly applicable to the discovery of novel nucleoside analog treatments for respiratory viruses. The review by Wiemer is of note since it discusses the relationship between metabolism properties of phosphoramidates and route of administration, which together contribute to the distribution of the phosphate payload in vivo.[7] This is highly relevant for the application of phosphoramidate prodrugs with respect to lung delivery as a relatively new advance in the nucleoside prodrug field. This work aims to review the published evidence supporting the ability of phosphoramidate prodrugs to deliver nucleoside monophosphates into lung cells in vitro and in vivo for the inhibition of RSV and other respiratory viruses. The journey of **1** serves as the key case study for lung delivery and highlights the importance of continued nucleoside prodrug research to discover novel antivirals for emerging respiratory viruses with pandemic potential.

The class of nucleoside-based antivirals (nucleosides and nucleoside phosphonates) are good examples of the delivery challenge highlighted in the opening paragraph that can be solved by utilizing prodrugs. The molecular targets of nucleoside-based antivirals are typically the viral RNA and DNA

polymerases that are delivered or expressed in an infected cell following attachment and entry of a viral particle, as illustrated in Figure 1. Viral polymerases are essential enzymes in the life cycle of a virus and serve to faithfully copy the viral DNA or RNA genome using the intracellular pools of natural nucleotides, for example, ATP, GTP, CTP, and UTP for RNA synthesis. The inhibitors in their respective triphosphate forms act as structural mimics of the natural nucleotide triphosphates, and "trick" the polymerase into recognizing and then incorporating the unnatural nucleotide analog into the nascent RNA or DNA instead of the natural nucleotide. For example, the bioactive inhibitor of prodrug **1** is its triphosphate, **1**-TP, a highly polar charged species with limited permeability that is a structural analog of ATP (Figure 1). It differs from ATP by the presence of the 1′-CN group and the 4-aza-7,9-dideaza C-adenine nucleobase instead of adenine. Inhibitor **1**-TP readily competes with ATP for incorporation of the nucleotide into the nascent viral RNA strand by the viral RdRp resulting in inhibition of full-length RNA replication. There are various mechanisms through which inhibition of full-length RNA synthesis occurs which will not be reviewed in great detail here. However, in brief, once the unnatural C-nucleotide is incorporated by the viral RdRp enzyme elongation can continue for several more nucleotides before synthesis is halted (delayed chain termination).[3,9] In addition, for SARS-CoV-2 it has been determined that full length RNA can be generated containing the unnatural nucleotide, but this daughter strand cannot serve as a reliable template (template-dependent inhibition).[10] Despite these different mechanisms following incorporation it can be appreciated that the driver of the desired pharmacodynamic effect in vivo is a combination of the active **1**-TP concentration in the virally infected lung cells, together with its inhibitory
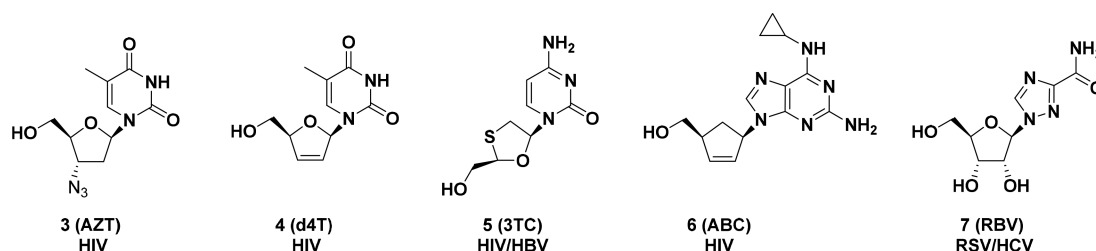
Figure 2. Selected examples of nucleoside antivirals. The compounds mimic the natural nucleosides; **3** and **4** (thymidine analogs), **5** (deoxycytosine), **6** (metabolized to a deoxyguanosine), and **7** (adenosine/guanosine).

Table 1. Anti-HCV Activity of Selected Ribonucleoside Analogs and Their Respective Phosphoramidate Prodrugs

compound	name	parent nucleoside HCV replicon (μM)[a]	monophosphate prodrug HCV replicon (μM)[a]	clinical status
8	PSI-7977 (sofosbuvir)	$EC_{50} > 50$	$EC_{90} = 0.42$	approved
9	INX-08189 (BMS-986094)[b]	$EC_{50} = 3.5$	$EC_{50} = 0.035$	Ph 2 stopped
10	GS-6620	$EC_{50} > 89$	$EC_{50} = 0.46$	Ph 1 stopped
11	AT-527 (bemnifosbuvir)[b]	$EC_{90} = 69$	$EC_{50} = 0.013$	Ph 2 ongoing
12	MK-3682, IDX-21437 (uprifosbuvir)	$EC_{50} = 57$	$EC_{50} = 0.32$[c]	Ph 2 stopped
13	AL-335		$EC_{50} = 0.07$	Ph 2 stopped

[a]See extended table in Supporting Information for antiviral activity references. [b]Parent nucleoside data is for the guanosine analog since the active triphosphate species is a guanosine triphosphate. [c]Performed in Ces1 expressing huh-7 cells.
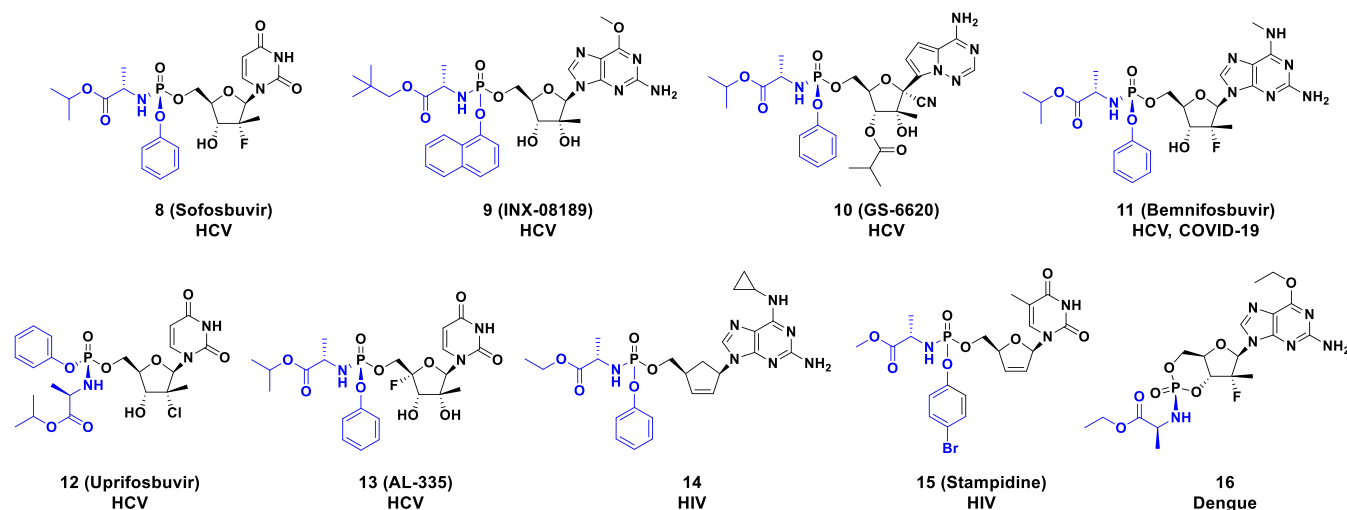
Figure 3. Phosphoramidate prodrugs targeting HCV, HIV, and dengue. The promoiety (blue) is cleaved to release the respective nucleoside monophosphate (black). Examples **8**, **10**, **11**, and **13** have *Sp* stereochemistry at phosphorus, **12** and **16** *Rp*, and the others undefined.

potency (i.e., concentration of TP required to inhibit 50% of viral replication). Since **1**-TP is ionized and poorly permeable, the in vivo cellular delivery of this charged triphosphate species becomes a key challenge for all nucleoside-based antiviral programs.

One strategy to deliver the TP inhibitor is to administer the neutral nucleoside analog, for example, **2**−**7** as shown in Figures 1 and 2. Following entry into a cell by passive permeation or nucleoside transporters, the nucleoside analog can harness host intracellular phosphorylating enzymes to generate the 5′-monophosphate, 5′-diphosphate, and ultimately, the active TP form. This strategy proved successful for teams engaged in the design of deoxyribonucleoside analogs, that is, analogs that mimic natural deoxyribonucleosides to target herpes DNA polymerase, HIV reverse transcriptase, or hepatitis B DNA polymerase resulting in the approval of multiple antiviral drugs, for example, AZT (**3**), d4T (**4**), 3TC (**5**), FTC, and abacavir (**6**) (Figure 2).[11,12] Shortly after 2000, nucleoside teams across the

industry, including Gilead, began deliberate efforts toward the design of ribonucleoside analogs to target viral RdRp enzymes as opposed to DNA polymerases, driven mostly by the hunt for a more effective HCV cure. At the time, the only FDA approved ribonucleoside antiviral was ribavirin, **7**, approved for the treatment of RSV and HCV, the latter only when used in combination with interferon. The key design consideration for novel HCV RdRp inhibitors was the inclusion of the requisite 2′-OH (or equivalent bioisostere, e.g., 2′-halo) on the ribose core to promote recognition of the analog as a ribonucleotide substrate. However, in our experience and we suspect those of many others, it proved challenging to identify novel ribonucleoside analogs that were potent inhibitors of the RdRp and at the same time retained efficient conversion by cellular phosphorylating enzymes. In general, as the number of structural changes on the nucleoside analog increased relative to the natural ribonucleosides, the risk of inefficient recognition and conversion by the host metabolizing enzymes also increased.

Table 2. Antiviral Potency of 1 and Parent Nucleoside 2 Across Multiple Viruses and Cell Types

virus	cell line[a]	compound 1 EC$_{50}$ (μM)	compound 2 EC$_{50}$ (μM)	fold difference[b]	ref
RSV	HEp-2	0.015	0.53	35	1
	NHBE	0.049	1.85	38	1
HCV	Huh-7	0.057	4.1	72	1, 13
Ebola	Macrophage	0.086	>20	>232	2, 3
	HeLa	0.14	>20	>143	2, 3
Marburg	Huh-7	0.014	1.9	136	5
Nipah M1999	HeLa	0.066	2.12	32	5
Nipah B2004	H358	0.032	2.46	77	5
Measles	HeLa	0.037	1.0	27	5
	HMVEC	0.06	0.77	13	5
SARS	HAE	0.069	0.18	2.6	4
SARS-CoV-2	A549-hACE2	0.115	0.869	7.6	24
	HAEC (HAE)	0.048	0.51	11	25
	Huh-7	<0.001	1.1−1.5	>1000	25
	Vero-E6[c]	0.74−1.65[d]	0.47−1.1[d]	0.7[e]	24−28
	Caco-2	0.001	0.08	80	26
	Calu-3	0.11	0.25	2.4	26
	Calu-3 2B4	0.28	0.62	2.2	27
	HAE	0.01			27
	PSC-human lung	0.14	0.74	5.3	28
MERS	Calu-3 2B4	0.069			4
	HAE	0.074	0.86	12	4

[a]Human cell line origin unless otherwise noted. [b]Fold difference is the ratio of EC$_{50}$ 2 to EC$_{50}$ 1. [c]African green monkey Vero-E6 cells. [d]Upper and lower range of data reported across multiple references. [e]Ratio reported as an average ratio derived from the calculated ratio of 1 and 2 reported in the same assay format.

For example, Table 1 shows the HCV activity of several nucleosides that were later clinically developed for HCV as their phosphoramidate prodrugs 8−13 (Figure 3). Weak antiviral activity was observed in HCV replicon cell-based assays for the parent nucleosides primarily due to poor conversion to their respective monophosphate metabolites, although poor permeability properties may also contribute to some extent.

Severe RSV infection carries a high risk of morbidity and mortality in vulnerable patients, especially premature infants and the elderly with underlying conditions such as COPD and asthma, or the immunosuppressed.[1] Like HCV, RSV has a viral RdRp enzyme and therefore was of interest within Gilead to explore in parallel to designing HCV RdRp inhibitors. Through screening our collection of HCV nucleoside analogs we identified the 1′-CN C-nucleoside 2 as a very promising lead with an RSV EC$_{50}$ = 0.53 μM, that was ~10-fold improved over its HCV activity (Table 2).[1,13] The triphosphate 1-TP was found in biochemical assays to be more potent toward RSV RdRp (IC$_{50}$ = 1.1 μM) compared to HCV RdRp (IC$_{50}$ = 5.6 μM), consistent with the improved antiviral activity in cells. These data resulted in the formation of an RSV nucleoside program with the initial aim of exploring the SAR around 2, optimizing the RSV potency of 1 especially in lung cells through prodrugs, and establishing RSV efficacy in vivo. The SAR to replace the 1′-CN with other functional groups, or modify other regions of the molecule proved to be very steep. For example, the corresponding 1′-alkyne analog had weaker RSV activity, and removal of the 1′-substituent altogether resulted in a very toxic compound.[1] Among the novel nucleoside analogs that were designed for RSV very few had potent activity in the HEp-2 cell assay, which was once again presumed to be due to the slow conversion to the monophosphate rather than permeability factors.[1,14] Indeed, since the start of our RSV nucleoside

program there are only a few sparse examples of potent RSV nucleoside analogs in cell culture reported in the literature.[15,16]

Faced with the intracellular metabolism challenge for many ribonucleoside analogs, methods to deliver the phosphorylated anabolites using prodrugs to mask the ionizable groups on the phosphates were considered. This strategy can bypass a rate-limiting phosphorylation step leading to improved cellular potency. In addition, the prodrug design can raise the lipophilicity of the nucleoside analog potentially improving its permeability. The inherent value of this approach should not be underestimated because it significantly expands the scope of nucleoside analog designs that can be considered as potential antivirals. Moreover, if the phosphate prodrug designs can favorably distribute the nucleoside monophosphate into certain cell types, for example, lung cells, then this strategy would allow more effective targeting of RSV and other respiratory viruses. Finally, since many emerging respiratory viruses are RNA viruses, including coronaviruses (SARS-CoV-1, MERS-CoV, SARS-CoV-2), paramyxoviruses (nipah, measles), and orthomyxoviruses (influenza), the development of prodrugs that can deliver phosphorylated ribonucleosides into lung cells has broad ranging implications with respect to building an arsenal of treatment options for future pandemic preparedness.

Several strategies to deliver the monophosphate nucleoside analogs have been described in the literature including thioester prodrugs (SATE), *cyclo*SAL, phospholipid, and amino acid-based prodrugs (phosphorodiamidates and phosphoramidates or ProTides), of which the latter was extensively studied by the late Professor McGuigan.[17−21] In his early phosphoramidate research, McGuigan applied the approach to HIV deoxynucleoside analogs, for example, AZT 3 and demonstrated antiviral activity superior to AZT in a cell line deficient in thymidine kinase required to convert AZT to its monophosphate. This result confirmed the phosphorylation bypass effect of the

phosphoramidate design in vitro.[20] The proposed promoiety breakdown pathway begins with an intracellular esterase mediated hydrolysis of the amino acid ester, cyclization to eject the aryloxy leaving group followed by hydrolysis to the alanine metabolite, and finally a phosphoramidase hydrolysis mediated by HINT-1 to release the monophosphate (Figure 1).[22] To target HCV, it was necessary to establish delivery of the ribonucleoside monophosphate analogs into hepatic cells in vitro and in vivo. Phosphoramidate prodrug 8 was found to improve potency in hepatic Huh-7 cells in vitro compared to its parent nucleoside, and in vivo, high levels of the active triphosphate species was measured in liver tissue fractions collected in preclinical species (Table 1). Following the development of 8, several other phosphoramidate prodrugs of HCV RdRp analogs 9−13 were identified with improved potency over their parent nucleosides, although 9 and 10 both failed in early trials due to safety and variable pharmacokinetics, respectively. These results established that some phosphoramidate prodrugs could effectively deliver monophosphate nucleoside analogs into hepatic cells in vitro and in vivo.

Although nucleoside 2 possessed antiviral activity for RSV supporting limited potential to metabolize to the active 1-TP in epithelial cells, it was projected to be too inefficient to be an effective, low dose, RSV inhibitor. This projection was based on the low predicted human oral bioavailability of 2 combined with the high systemic exposure of 2 that was required to generate lung tissue levels of 1-TP that exceeded the RSV IC_{50} of 1.1 μM (see later discussion). We, therefore, explored a monophosphate prodrug approach to improve the potency of the lead 2 toward RSV in lung epithelial cells and more effectively generate 1-TP in lung tissue. To start the prodrug effort at least several of the monophosphate options mentioned above were evaluated including SATE, phosphorodiamidates, and aryloxy phosphoramidates. We discovered that the single diastereoisomer Sp monophenol isopropyl alanine ester prodrug, the same promoiety reported in 8 and other amidates (Figure 2), had a 1.5-fold improved potency over 2 in the RSV HEp-2 (cervical epithelial cell) assay.[1] However, this prodrug was found to be quite polar (log D = 1.1), due to the polar nucleoside parent bearing both hydroxyls and a 1′-CN group. We hypothesized that the polarity may be limiting cell permeability and esterase conversion inside cells, so we increased the lipophilicity by modifying the ester group and found that the 2-ethylbutylalanine ester, 1 (log D = 2.5), was 20-fold more potent than the corresponding isopropylalanine ester and 35-fold improved over 2 (Table 2).

A key consideration during phosphoramidate prodrug discovery is that the prodrug breakdown is by host enzymes, not viral enzymes, and therefore, expected to be cell/tissue specific. Potency is presumably correlated with expression levels of metabolizing enzymes, and the activity of the prodrug toward these enzymes, for example, Ces1/2 and Cat A as examples of esterases, and HINT1 for the hydrolysis of the alanine metabolite (Figure 1). To demonstrate that 1 was effectively activated in primary lung cells, RSV assays were developed in primary normal human bronchial epithelial cells (NHBE) that are precursors to the ciliated epithelial cells, and also the human airway epithelial (HAE) culture model, considered by many to be the best in vitro representation of the human lung. The RSV phosphoramidate SAR in NHBE cells proved to be very similar to that observed in HEp-2 cells, with 1 demonstrating a comparable 38-fold greater potency over 2 (Table 2).[1] In a RSV HAE culture assay, which detected viral RNA changes by PCR, 1

was also more potent than parent nucleoside 2 by an estimated ~40-fold. Therefore, it was clearly demonstrated that 1 could be effectively cleaved and activated to 1-TP in primary lung cells. As the RSV nucleoside program progressed, the phosphoramidate prodrug strategy was successfully applied to other C-ribonucleoside analogs.[14]

Compound 1 was not selected for clinical development toward RSV in favor of developing an alternative nucleoside series that demonstrated broad activity toward several common respiratory viruses. Strategically, a product with broad activity toward RSV and other respiratory viruses such as human rhinovirus or influenza, affords an opportunity to benefit more patients that are at risk due to respiratory infections. The West Africa Ebola outbreak began after the start of our RSV program, and in response to the crisis, we screened compounds from our ribonucleoside library in collaboration with the CDC and USAMRIID and showed that 1 was a highly potent inhibitor of Ebola in HMVEC, HeLa, and macrophage cell lines, the latter cell line reflecting what was thought to be a primary site of viral replication in the early stages of human disease (Table 2).[2,3] This demonstrated that 1 was also effectively metabolized in nonlung cell types. Although 1 had already been identified, we chose to rapidly expand the suite of prodrugs as was described by Siegel et al.[2] However, no improved phosphoramidate prodrugs were discovered for Ebola, although several were close in potency to 1 in the HMVEC cell line. It was notable that the aforementioned Sp isopropyl alanine ester analog, which was >20-fold less active than 1 in the RSV HEp-2 and NHBE cell assays, was only 3.5-fold less active than 1 toward Ebola in macrophages. The smaller difference in the relative potencies is presumed to be due to the isopropyl alanine ester being a preferred substrate for different intracellular esterases compared to 1, that in turn, are differentially expressed across macrophages and lung cells.[23] Further investigation of the enzymes metabolizing the isopropyl alanine ester would be required to confirm this, but the key conclusion was that these data emphasize the importance of conducting antiviral prodrug optimization in the relevant target cell types. Testing of 1 toward other emerging RNA viruses, including numerous respiratory viruses was also conducted and showed that 1 had broad-spectrum activity across multiple RNA viruses replicating in different human lung and non-lung cell types with EC_{50} values in most cell types below 150 nM (Table 2).[24−28] Notably, high potency was established toward the coronaviruses MERS-CoV and SARS-CoV-1 in HAE cells, and more recently toward SARS-CoV-2 across multiple lung cell lines including A549-hACE2, human pluripotent stem cell derived lung cells, and HAE cell cultures. Weak potency toward SARS-CoV-2 was observed in Vero E6 cells (African Green Monkey kidney cells) because this cell line does not efficiently convert 1 into 1-TP.[26,27] Turning to the parent nucleoside 2, the activity was more variable across the same antiviral assays and in some cell-types, such as macrophages, huh-7, and H358 cells, it is considerably less potent than 1 (Table 2). This is presumably the result of slow metabolism of 2 into 1-MP due to reduced expression of intracellular kinases, such as adenosine kinase combined with any permeability differences. For example, the activity of 2 against Ebola in macrophages, where the expression level of adenosine kinase is generally lower than epithelial lung cells, was significantly weaker than 1 which contributed to the decision to develop 1 for Ebola.[23] In some lung cells (HAE, A549-hACE2, and Calu-3), the relative potency difference between 1 and 2 is not as high but still favors 1 by 2.6-fold to 12-fold for SARS, SARS-CoV-2, and

Table 3. Plasma Pharmacokinetics of Representative Phosphoramidate Prodrugs in Nonrodent Species

compound	species	dose (mg/kg)	route	IV CL (L/h/kg)	IV $T_{1/2}$ (min)	IV V_{ss} (L/kg)	plasma prodrug AUC_{0-inf} (μM h)	plasma nucleoside AUC_{0-last} (μM h)	F%	lung TP@24 h (nmol/g tissue)	ref
8	cyno	5	oral				0.16	0.12			30
9	cyno[a]	30	oral				0.026				31
11	cyno[a]	30	oral				0.44	1.56		(0.14 μM)[b]	33
14	cyno	11.5	IV	6.8	6.6	n.d.	2.7	6.0			29
14	cyno	11.5	oral				0.7	6.0	22		29
8	dog	5	oral				0.78	27			30
10	dog	0.5	oral				0.16				32
15	dog	100	oral				23.1	262			34
16	dog	0.5	IV		18	0.5	0.61				35
16	dog	3	oral				1.6		44		35
1	ferret	10	IV	2.6	11	0.34	7.0	18.2		1.28	36
1	rhesus	10	IV		23						3,37
1	cyno	10	IV	1.92	24	0.45	8.8	8.7		1.39	1
1	AGM	10	IV	2.13	48	0.94	7.9	8.4		1.03	1
1	human[c]	2.5	IV	0.86	60	1.22	5.0	7.5			38

[a]Data reported after a multidose regimen. [b]Data was reported in micromolar. [c]Assumes a 60 kg adult. n.d.: Not determined. V_{ss}: Volume at steady state. inf: Infinity.

MERS, and closer to ~40-fold for RSV in our assays.[1] The fold difference in HAE cells would probably be more similar if the assays were conducted in parallel, but it is likely that donor–donor variability results in the wide-ranges observed. Overall, the phosphoramidate prodrug 1 demonstrates potent broad-spectrum antiviral activity in vitro that is superior to 2 across all the human lung and non-lung cell types tested, including many types of primary cells. The promoiety design of 1 is, therefore, more effective than parent 2 at generating 1-MP across multiple different cell types in vitro.

The ability to quantify the intracellular TPs, including the intermediates in the prodrug breakdown, has been an important technical advance in the nucleoside field over the past 20 years that has enabled the optimization and development of many antiviral nucleoside analogs. Beyond correlating increased antiviral potency with increased intracellular TP levels, the technique can provide insight into TP formation kinetics, allow an estimate of TP content when virus replication is inhibited by 50% in cells (intracellular IC_{50} assessment of the TP potency), and provide an understanding of intracellular TP half-life. The technique can be applied to in vitro culture systems but also tissue samples harvested from in vivo experiments. These studies are critically important for accurate in vitro to in vivo translation and informing on the pharmacokinetic/pharmacodynamic (PK/PD) relationship that enables human dose and dosing regimens to be projected.

To confirm that the improved antiviral activity in vitro of 1 is the result of increased levels of 1-TP relative to 2, intracellular metabolism studies were conducted in the cell lines of the RSV assays.[1] Continuous incubation of 1 in the HEp-2 and NHBE cells at 1 μM resulted in average 1-TP levels over 48 h of 20.5–22 pmol/million cells, 10–20-fold higher than the levels generated from 2 (0.9–2.0 pmol/million cells), under the same conditions. The >20-fold elevated 1-TP levels following the incubation of 1 is consistent with the >35-fold improved anti-RSV activity that was observed in these cell types. Estimating the average levels of 1-TP over 48 h that would have been generated if the incubations were conducted at the respective RSV EC_{50} concentrations (i.e., 0.049 μM for 1 and 1.85 μM for 2 in NHBE cells in Table 2) affords an estimate of the 1-TP concentration that results in 50% inhibition of viral

replication. These calculations from the HEp-2 and NHBE metabolism studies resulted in an estimated concentration of 1-TP ranging from 0.1–0.35 μM toward RSV, within close approximation of the experimentally determined IC_{50} toward the RSV RdRp complex in a biochemical assay (IC_{50} = 1.1 uM).[1] An under-appreciated advantage of the intracellular IC_{50} estimation for viral inhibition is its utility in informing on target TP levels in cells when a biochemical polymerase assay is unavailable, as was the case for Ebola, where an intracellular IC_{50} was estimated to be ~5 μM for inhibition of Ebola replication.[3] Later, an IV dose of 10 mg/kg 1 in rhesus monkeys was found to generate >5 μM 1-TP concentrations in peripheral blood mononuclear cells (PBMCs) at 24 h leading to the selection of this dose as the initial loading dose in the subsequent Ebola efficacy studies.[3] Finally, the half-life of 1-TP can also be determined by conducting a short incubation of 1, to allow TP to form, followed by removal of the prodrug and extracellular metabolites by washing, and then following the TP decay kinetics over time. The half-life of 1-TP in human macrophages and NHBE cells was ~14 h supporting once daily administration for Ebola and the suitability for the same daily dosing schedule for the treatment of SARS-CoV-2.[1,3] Thus, the nucleoside metabolism data generated in vitro and in vivo for the phosphoramidate prodrugs can correlate the improved antiviral activity with increased TP formation as a result of monophosphate delivery but also inform on dose levels and dose frequency in vivo.

The improved antiviral activity of 1 and 1-TP formation in primary lung cells, combined with its long ~14 h intracellular half-life, provided the foundation to address whether the phosphoramidate approach could effectively deliver 1-MP into lung cells in vivo to generate 1-TP and anti-RSV efficacy. Consistent with the lack of in vitro evidence for lung cell delivery and TP formation by phosphoramidates, there were no reports that we were aware of at the time demonstrating in vivo delivery of a monophosphate nucleoside into lung cells concurrent with in vivo antiviral efficacy. To establish proof-of-concept for lung distribution by the phosphoramidates, plasma exposure of intact prodrug was considered important. However, upon reviewing the available phosphoramidate literature, it was clear that the majority of the in vivo preclinical pharmacokinetic (PK) data

reported at the time was focused on phosphoramidates orally delivering nucleoside monophosphates into the liver to target HCV. Rodents were heavily utilized in these studies to allow frequent collection of liver tissue samples and evaluation of hepatic intracellular TP formation. However, because of the high plasma esterase activity in rodents, the plasma exposures of the prodrugs are extremely low in rodents (mouse plasma $t_{1/2} < 5$ min for **1**) and not reflective of higher species.[4] One report was identified that described the intravenous (IV) pharmacokinetics in cynomolgus monkey for the HIV phosphoramidate prodrug **14**, which showed rapid clearance and a short plasma half-life of 6.6 min (Table 3).[29] This suggested rapid breakdown of the promoiety in the liver and likely additional breakdown in plasma and other nonhepatic tissues since the clearance exceeded liver blood flow. Nonrodent plasma PK data has now been reported for **1**, and several phosphoramidate prodrugs that target HCV, HIV, and dengue as shown in Table 3.

Oral optimization was not purposefully conducted to identify **1** as it was predicted and later confirmed in cynomolgus monkey that oral bioavailability was very low at F < 1%.[1] In vivo studies on **1** following IV administration demonstrated a half-life of 11–60 min across multiple species, longer than the half-life reported for **14** in dogs. As noted earlier in rhesus, IV dosing of **1** resulted in delivery of the monophosphate nucleoside and efficient formation of **1**-TP at micromolar concentrations in PBMCs.[3] This result established that despite the short systemic exposure of the prodrug **1**, it could distribute from the plasma compartment into tissues other than the liver. Prodrug **16** also is reported to have a longer half-life in dogs than **14** and its active triphosphate was similarly detected in PBMCs in vivo.[35] Prodrug **1** has a favorable steady state volume of distribution across species, reflective of the moderate lipophilicity of **1**, and the potential for rapid distribution into tissues beyond PBMCs such as the lung. In clinical studies, the half-life and volume of distribution for **1** was approximately the same as that observed in nonhuman primates (NHPs), suggesting that NHPs are a good model for studying the distribution of **1** and formation of **1**-TP in lung tissue. Following IV dosing, gross lung tissue samples were surgically extracted at 24 h in both cynomolgus and AGMs and a consistent level of **1**-TP (~3 μM or ~1–1.4 nmol/g lung tissue) was shown at 24 h confirming that **1** was able to effectively distribute into and metabolize in lung tissues (Table 3). Lung **1**-TP levels have also been observed from short plasma exposures of **1** in the lungs of ferrets, following IV administration, and also the lungs of Ces1c$^{-/-}$ engineered mice, following subcutaneous administration of **1** (plasma half-life was 25 min).[4,36] Thus, the in vivo ability of **1** to deliver **1**-MP into lung cells, and then efficiently form **1**-TP, has been demonstrated in multiple preclinical species despite a relatively short plasma half-life of <1 h. Furthermore, the approximately equivalent plasma exposure of **1** in the plasma of ferret, cynomolgus monkey, and AGM resulted in comparable lung **1**-TP levels at 24 h, across these species suggesting that the promoiety is broken down, and **1**-MP metabolized, similarly across multiple nonclinical species. Finally, lung TP formation has recently been reported for phosphoramidate **11** delivered orally and supports its progression into clinical studies for COVID-19.[33] Taken together these studies confirm that short duration systemic exposures of phosphoramidate prodrugs, if suitably designed, can effectively deliver nucleoside monophosphate into the lungs in vivo and generate the desired TP.

The observation that **1**-TP is present in lung at 24 h, despite the rapid elimination of the prodrug during the first few hours

following IV dosing, has fueled some speculation by Yan and co-workers that it is not the prodrug that drives **1**-TP formation, but instead, parent **2** that is also observed in plasma as the main metabolite with a more prolonged half-life (Table 3; plasma nucleoside **2** has similar AUC to that of prodrug).[39] This hypothesis is supported by in vitro data demonstrating **2** has antiviral activity in lung cells and some, albeit limited, in vitro metabolism.[1,27] However, an in vivo assessment of lung metabolism for **2** at a time point of 24 h was conducted within the RSV program and more recently reconfirmed in a direct metabolism study comparing **1** and **2** in cynomolgus monkey.[1] A high 20 mg/kg IV dose of parent nucleoside **2** was shown to result in a 4-fold lower lung **1**-TP level compared to that derived from a 4-fold lower molar IV dose of 10 mg/kg of **1**. Plasma PK confirmed that the dose of **2** resulted in a much higher C_{max} and exposure of **2** compared to the level of **2** in plasma that is derived from **1** (66-fold higher C_{max} concentration and 14-fold higher AUC_{0-24} exposure).[1] Taken together, it can be concluded that the lung **1**-TP following IV administration of **1** is predominantly driven from the systemic exposure to **1**, and not **2**. The lower **1**-TP concentration despite the ~4-fold higher molar dose administered of **2**, means that in cynomolgus monkey the phosphoramidate **1** is ~15-fold more efficient at generating **1**-TP in lung than **2** on a molar equivalent dose basis. Consistent with these data >10-fold efficiency of **1** for lung loading of **1**-TP in AGM and ferrets was estimated from recently reported studies in these species.[1,36] Several properties support the ability of **1** to effectively deliver **1**-TP despite its short plasma exposure. First, its facile distribution into lung cells from circulation based on its moderate lipophilicity as evidenced by the volume of distribution. Second, rapid esterase metabolism in lung cells generates the initial acid metabolite that is then "trapped" inside the cell since it, and all the subsequent key metabolic species en-route to **1**-TP, are ionized and have limited passive leakage out of the cell during conversion to **1**-TP (see Figure 1). Finally, the long intracellular TP half-life of ~14 h established in NHBE cells in vitro permits persistent levels of **1**-TP to be observed at 24 h despite the absence of prodrug in the circulation.[1] The proof-of-concept lung data reported for **1** across multiple species in vivo supports the conclusion that this phosphoramidate promoiety is effective at bypassing the limited metabolism of **2** in lung cells in order to achieve good lung delivery of **1**-TP. To this end, nucleoside analogs beyond **2** that also have weak antiviral activity for a given respiratory virus due to limited metabolism may also be suitable candidates for a similar phosphate prodrug approach.

For any given phosphoramidate prodrug, it is expected that it would be metabolized at different rates across cell-types due to differential enzyme expression and activity of the metabolizing enzymes, so it should not be assumed that all lung cell types in a given lung tissue sample will have the same concentration of TP. Metabolism studies of tissue samples cannot determine TP concentrations at a single cell-type level due to the inherent instability of the TP species. Within Gilead, this technical hurdle has prompted consideration of other methods for the collection of specific lung cells or different methods for analyzing the intracellular metabolites. However, an indirect method for confirming the TP is generated in the diseased cells is to use animal efficacy models. We, therefore, chose to evaluate **1** in the RSV AGM model using daily IV administration at 10 mg/kg, the dose that was established for the Ebola in vivo efficacy studies. On the basis of the AGM lung metabolism data this dose produces ~3 μM of **1**-TP at 24 h in the lungs of AGMs, an order

Table 4. Respiratory Virus Efficacy Models Conducted with 1[a]

virus	species	Dose (mg/kg, regimen[b])	route[c]	summary of results[d]
RSV A2	AGM	10, QD	IV	decreased lung and nasopharyngeal VL
Nipah	AGM	10, QD	IV	100% survival
MERS-CoV	Rhesus	5, QD	IV	decreased lung VL, decreased clinical signs
MERS-CoV	Ces1c$^{-/-}$ hDPP4 mice	25, BID	SC	decreased lung VL, decreased clinical signs
SARS-CoV-1	Ces1c$^{-/-}$ mice	25, BID	SC	decreased lung VL, decreased clinical signs
SARS-CoV-2[e]	Ces1c$^{-/-}$ mice	25, BID	SC	decreased lung VL, decreased clinical signs
SARS-CoV-2	rhesus	10/5, QD	IV	decreased lung VL, decreased clinical signs

[a]See Supporting Information for extended table with references. [b]QD: Once daily. BID: Twice daily. [c]IV: Intravenous. SC: Subcutaneous. [d]VL: Viral load. [e]SARS-CoV-1 chimeric virus with SARS-CoV-2 RdRp.

of magnitude higher than the **1**-TP concentration that was estimated to inhibit 50% viral RSV replication in human NHBE cells. Dosing of **1** beginning 4 h before infection (to allow some time for **1**-TP to develop in the lung tissue), demonstrated a strong >2-log reduction in lung viral load in lavage samples relative to vehicle control animals, confirming an antiviral effect of the phosphoramidate prodrug (Table 4) consistent with the formation of **1**-TP in the lung.[1]

We also explored the efficacy of **1** toward SARS-CoV-1 in Ces1c$^{-/-}$ mice and in this mouse model, 25 mg/kg twice daily subcutaneous administration was effective at reducing the lung viral titer through day 5 when dosing was initiated 1 day before innoculation (prophylactic), and to a lesser extent, when dosing was initiated 1 day after infection (treatment).[4] Taken together, these efficacy models in AGM and Ces1c$^{-/-}$ mice established an antiviral effect in the lung consistent with the presence of **1**-TP in the lung tissue metabolism studies. Since conducting these early efficacy studies, a growing body of evidence for the antiviral efficacy of **1** toward other respiratory pathogens including MERS-CoV (Ces1c$^{-/-}$ hDPP4 mice and rhesus), nipah (AGM), and more recently SARS-CoV-2 (Ces1c$^{-/-}$ mice, rhesus, AGM) has been reported (see Supporting Information for references). This substantive body of efficacy data further adds weight to the ability of **1** to effectively deliver the monophosphate nucleoside into lung cells relevant for viral infections leading to efficient formation of **1**-TP. The SARS-CoV-2 efficacy data also supported the clinical development of **1** for SARS-CoV-2, but it should be noted that the translational value to human disease of many of these efficacy models is not fully understood. For example, human RSV infection in nonhuman primates other than chimpanzees results in minimal clinical disease and, therefore, does not fully recapitulate the human disease.[40]

The IV route of administration for **1** was suitable for proof-of-concept studies and is an acceptable route of administration in the hospital setting but inconvenient in an outpatient setting. More convenient routes of administration include subcutaneous injection, intramuscular injection, inhalation, or oral delivery. The efficacy studies in Ces1c$^{-/-}$ mice utilized subcutaneous injection of **1** suggesting this is a viable option for delivery of the phosphoramidate into systemic circulation. Further, in response to the current pandemic an inhaled formulation of **1** was developed leading to the initiation of clinical trials in 2020. The direct delivery to the lung has some potential advantages over oral systemic delivery if the virus is mainly replicating in the lung, including more rapid delivery and onset of action in the lungs and reduced systemic exposure of prodrug and metabolites. Dose limitations are however practical challenges for both subcutaneous and inhaled delivery due to limited dose volume of an injectable, or the device and duration of device interaction

required for inhaled delivery. Oral delivery is perhaps the most preferred route of administration and preclinical oral data reported for phosphoramidates **14** and **16** is quite encouraging with oral bioavailabilities of 22% in cynomolgus monkey and 44% in dog, respectively (Table 3). Indeed phosphoramidate **11** is the second phosphoramidate prodrug to be explored for COVID-19 in the clinic and is delivered orally. Taken together, oral phosphoramidate prodrugs that result in plasma prodrug exposures compatible with favorable lung TP formation to support efficacy may be feasible.

There is still much to learn regarding the lung delivery of antiviral nucleoside monophosphates using phosphoramidate prodrugs, including options for potential tissue-selective prodrug activation based on an improved understanding of target cell/tissue metabolic pathways. Such efforts may well lead to improved prodrug designs in the future. Also, the assessment of alternate routes of administration that are more convenient will enable more effective therapies with broad patient access. The current COVID-19 pandemic continues to impact many regions of the world through novel variants, and the risk for future respiratory pandemics by novel emerging viruses is well-recognized now. Since many nucleoside analogs are approved drugs for the treatment of both chronic and acute viruses bringing along potential benefits of broad-spectrum activity and high barriers to resistance, further exploration of novel phosphate prodrug approaches is clearly a valuable investment to combat respiratory virus pandemics. The journey of **1** to FDA approval spanned more than a decade and traversed several different RNA viruses and disease indications as its broad-spectrum activity was uncovered. The initial discovery of the HCV nucleoside analog **2** as a promising RSV lead, followed by a prodrug campaign to deliver the polar monophosphate **1**-MP into lung cells and bypass a slow first phosphorylation step, resulted in the discovery of phosphoramidate **1** as a potent RSV inhibitor. By combining metabolism studies in vitro and in vivo with in vivo efficacy models across multiple preclinical species, it has been shown that **1** can effectively increase the levels of the active triphosphate **1**-TP in primary lung cells resulting in antiviral efficacy toward RSV and multiple other respiratory viruses. To date, more than 9 million hospitalized patients suffering from COVID-19 have been treated with **1**.

■ ASSOCIATED CONTENT

Ⓢ Supporting Information

The Supporting Information is available free of charge at https://pubs.acs.org/doi/10.1021/acsmedchemlett.1c00624.

Extended versions of Tables 1 and 4 with literature reference information added (PDF)

■ AUTHOR INFORMATION

Corresponding Author

   Richard L. Mackman − *Gilead Sciences, Inc., Foster City, California 94404, United States;* ● orcid.org/0000-0001-8861-7205; Email: rmackman@gilead.com

Complete contact information is available at:
https://pubs.acs.org/10.1021/acsmedchemlett.1c00624

Notes

The author declares the following competing financial interest(s): Richard Mackman is an employee of Gilead Sciences and may hold stock in the company.

■ ABBREVIATIONS USED

AGM, African green monkey; AUC, area under curve; CES1/2, carboxyesterase 1 or 2; COVID-19, coronavirus disease-2019; HAE, human airway epithelial; HCV, hepatitis C; HINT-1, histidine triad nucleotide-binding protein 1; HIV, human immunodeficiency virus; MP, monophosphate; NHBE, normal human bronchial epithelial; NHP, nonhuman primate; PBMC, peripheral blood mononuclear cell; RdRp, RNA-dependent RNA polymerase; RSV, respiratory syncytial virus; SARS, severe acute respiratory syndrome; SATE, *S*-acyl 2-thioethyl; TP, triphosphate

■ REFERENCES

(1) Mackman, R. L.; Hui, H. C.; Perron, M.; Murakami, E.; Palmiotti, C.; Lee, G.; Stray, K.; Zhang, L.; Goyal, B.; Chun, K.; Byun, D.; Siegel, D.; Simonovich, S.; Du Pont, V.; Pitts, J.; Babusis, D.; Vijjapurapu, A.; Lu, X.; Kim, C.; Zhao, X.; Chan, J.; Ma, B.; Lye, D.; Vandersteen, A.; Wortman, S.; Barrett, K. T.; Toteva, M.; Jordan, R.; Subramanian, R.; Bilello, J. P.; Cihlar, T. Prodrugs of a 1′-CN-4-Aza-7,9-dideazaadenosine *C*-Nucleoside Leading to the Discovery of Remdesivir (GS-5734) as a Potent Inhibitor of Respiratory Syncytial Virus with Efficacy in the African Green Monkey Model of RSV. *J. Med. Chem.* **2021**, *64* (8), 5001−5017.

(2) Siegel, D.; Hui, H. C.; Doerffler, E.; Clarke, M. O.; Chun, K.; Zhang, L.; Neville, S.; Carra, E.; Lew, W.; Ross, B.; Wang, Q.; Wolfe, L.; Jordan, R.; Soloveva, V.; Knox, J.; Perry, J.; Perron, M.; Stray, K. M.; Barauskas, O.; Feng, J. Y.; Xu, Y.; Lee, G.; Rheingold, A. L.; Ray, A. S.; Bannister, B.; Strickley, R.; Swaminathan, S.; Lee, W. A.; Bavari, S.; Cihlar, T.; Lo, M. K.; Warren, T. K.; Mackman, R. L. Discovery and Synthesis of a Phosphoramidate Prodrug of a Pyrrolo[2,1-*f*][triazin-4-amino] Adenine *C*-Nucleoside (GS-5734) for the Treatment of Ebola and Emerging Viruses. *J. Med. Chem.* **2017**, *60* (5), 1648−1661.

(3) Warren, T. K.; Jordan, R.; Lo, M. K.; Ray, A. S.; Mackman, R. L.; Soloveva, V.; Siegel, D.; Perron, M.; Bannister, R.; Hui, H. C.; Larson, N.; Strickley, R.; Wells, J.; Stuthman, K. S.; Van Tongeren, S. A.; Garza, N. L.; Donnelly, G.; Shurtleff, A. C.; Retterer, C. J.; Gharaibeh, D.; Zamani, R.; Kenny, T.; Eaton, B. P.; Grimes, E.; Welch, L. S.; Gomba, L.; Wilhelmsen, C. L.; Nichols, D. K.; Nuss, J. E.; Nagle, E. R.; Kugelman, J. R.; Palacios, G.; Doerffler, E.; Neville, S.; Carra, E.; Clarke, M. O.; Zhang, L.; Lew, W.; Ross, B.; Wang, Q.; Chun, K.; Wolfe, L.; Babusis, D.; Park, Y.; Stray, K. M.; Trancheva, I.; Feng, J. Y.; Barauskas, O.; Xu, Y.; Wong, P.; Braun, M. R.; Flint, M.; McMullan, L. K.; Chen, S. S.; Fearns, R.; Swaminathan, S.; Mayers, D. L.; Spiropoulou, C. F.; Lee, W. A.; Nichol, S. T.; Cihlar, T.; Bavari, S. Therapeutic Efficacy of the Small Molecule GS-5734 Against Ebola Virus in Rhesus Monkeys. *Nature* **2016**, *531*, 381−385.

(4) Sheahan, T. P.; Sims, A. C.; Graham, R. L.; Menachery, V. D.; Gralinski, L. E.; Case, J. B.; Leist, S. R.; Pyrc, K.; Feng, J. Y.; Trantcheva, I.; Bannister, R.; Park, Y.; Babusis, D.; Clarke, M. O.; Mackman, R. L.; Spahn, J. E.; Palmiotti, C. A.; Siegel, D.; Ray, A. S.; Cihlar, T. C.; Jordan, R.; Denison, M. R.; Baric, R. S. Broad-Spectrum Antiviral GS-5734 Inhibits Both Epidemic and Zoonotic Coronaviruses. *Sci. Trans. Med.* **2017**, *9* (396), No. eaal3653.

(5) Lo, M. K.; Jordan, R.; Arvey, A.; Sudhamsu, J.; Shrivastava-Ranjan, P.; Hotard, A. L.; Flint, M.; McMullan, L. K.; Siegel, D.; Clarke, M. O.; Mackman, R. L.; Hui, H. C.; Perron, M.; Ray, A. S.; Cihlar, T.; Nichol, S. T.; Spiropoulou, C. F. GS-5734 and its Parent Nucleoside Analog Inhibit Filo-, Pneumo-, and Paramyxoviruses. *Sci. Rep.* **2017**, *7*, No. 43395.

(6) Mehellou, Y.; Rattan, H. S.; Balzarini, J. The ProTide Prodrug Technology: From the Concept to the Clinic. *J. Med. Chem.* **2018**, *61* (6), 2211−2226.

(7) Wiemer, A. J. Metabolic Efficacy of Phosphate Prodrugs and the Remdesivir Paradigm. *ACS Pharmacol. Transl. Sci.* **2020**, *3* (4), 613−626.

(8) Slusarczyk, M.; Serpi, M.; Pertusati, F. Phosphoramidates and Phosphonamidates (ProTides) with Antiviral Activity. *Antivir. Chem. Chemother.* **2018**, *26*, No. 204020661877524.

(9) Gordon, C. J.; Tchesnokov, E. P.; Woolner, E.; Perry, J. K.; Feng, J. Y.; Porter, D. P.; Götte, M. Remdesivir is a Direct-Acting Antiviral that Inhibits RNA-Dependent RNA Polymerase From Severe Acute Respiratory Syndrome Coronavirus 2 with High Potency. *J. Biol. Chem.* **2020**, *295* (20), 6785−6797.

(10) Tchesnokov, E. P.; Gordon, C. J.; Woolner, E.; Kocinkova, D.; Perry, J. K.; Feng, J. Y.; Porter, D. P.; Götte, M. Template-dependent Inhibition of Coronavirus RNA-dependent RNA Polymerase by Remdesivir Reveals a Second Mechanism of Action. *J. Biol. Chem.* **2020**, *295* (47), 16156−16165.

(11) De Clercq, E. The Nucleoside Reverse Transcriptase Inhibitors, Nonnucleoside Reverse Transcriptase Inhibitors, and Protease Inhibitors in the Treatment of HIV Infections (AIDS). *Adv. Pharmacol.* **2013**, *67*, 317−358.

(12) Menéndez-Arias, L.; Álvarez, M.; Pacheco, B. Nucleoside/nucleotide Analog Inhibitors of Hepatitis B Virus Polymerase: Mechanism of Action and Resistance. *Curr. Opin. Virol.* **2014**, *8*, 1−9.

(13) Cho, A.; Saunders, O. L.; Butler, T.; Zhang, L.; Xu, J.; Vela, J. E.; Feng, J. Y.; Ray, A. S.; Kim, C. U. Synthesis and Antiviral Activity of a Series of 1′-Substituted 4-Aza-7,9-dideazaadenosine *C*-nucleosides. *Bioorg. Med. Chem. Lett.* **2012**, *22* (8), 2705−2707.

(14) Clarke, M. O. H.; Doerffler, E.; Mackman, R. L.; Siegel, D. (Gilead Sciences) Pyrrolo[1,2,f][1,2,4] Triazines Useful for Treating Respiratory Syncytial Virus Infections. WO2015/069939, 2015.

(15) Clarke, M. O.; Mackman, R.; Byun, D.; Hui, H.; Barauskas, O.; Birkus, G.; Chun, B.-K.; Doerffler, E.; Feng, J.; Karki, K.; Lee, G.; Perron, M.; Siegel, D.; Swaminathan, S.; Lee, W. Discovery of *β*-D-2′-Deoxy-2′-*α*-fluoro-4′-*α*-cyano-5-aza-7,9-dideazaadenosine as a Potent Nucleoside Inhibitor of Respiratory Syncytial Virus With Excellent Selectivity Over Mitochondrial RNA and DNA Polymerases. *Bioorg. Med. Chem. Lett.* **2015**, *25* (12), 2484−2487.

(16) Jordan, P. C.; Stevens, S. K.; Deval, J. Nucleosides For the Treatment of Respiratory RNA Virus Infections. *Antivir. Chem. Chemother.* **2018**, *26*, No. 204020661876448.

(17) Egron, D.; Imbach, J.-L.; Gosselin, G.; Aubertin, A.-M.; Périgaud, C. *S*-Acyl-2-thioethyl Phosphoramidate Diester Derivatives as Mono-nucleotide Prodrugs. *J. Med. Chem.* **2003**, *46* (21), 4564−4571.

(18) Meier, C.; Balzarini, J. Application of the *CycloSal*-prodrug Approach for Improving the Biological Potential of Phosphorylated Biomolecules. *Antivir. Res.* **2006**, *71* (2−3), 282−292.

(19) Hostetler, K. Y.; Stuhmiller, L. M.; Lenting, H. B.; van den Bosch, H.; Richman, D. D. Synthesis and Antiretroviral Activity of Phospholipid Analogs of Azidothymidine and other Antiviral Nucleosides. *J. Biol. Chem.* **1990**, *265* (11), 6112−6117.

(20) McGuigan, C.; Pathirana, R. N.; Balzarini, J.; De Clercq, E. Intracellular Delivery of Bioactive AZT Nucleotides by Aryl Phosphate Derivatives of AZT. *J. Med. Chem.* **1993**, *36* (8), 1048−1052.

(21) McGuigan, C.; Madela, K.; Aljarah, M.; Bourdin, C.; Arrica, M.; Barrett, E.; Jones, S.; Kolykhalov, A.; Bleiman, B.; Bryant, K. D.; Ganguly, B.; Gorovits, E.; Henson, G.; Hunley, D.; Hutchins, J.; Muhammad, J.; Obikhod, A.; Patti, J.; Walters, R. C.; Wang, J.; Vernachio, J.; Ramamurty, C. V. S.; Battina, S. K.; Chamberlain, S. Phosphorodiamidates as a Promising New Phosphate Prodrug Motif

for Antiviral Drug Discovery: Application to Anti-HCV Agents. *J. Med. Chem.* **2011**, *54* (24), 8632−8645.

(22) Siddiqui, A. Q.; McGuigan, C.; Ballatore, C.; Zuccotto, F.; Gilbert, I. H.; De Clercq, E.; Balzarini, J. Design and Synthesis of Lipophilic Phosphoramidate d4T-MP Prodrugs Expressing High Potency Against HIV in Cell Culture: Structural Determinants for in Vitro Activity and QSAR. *J. Med. Chem.* **1999**, *42* (20), 4122−4128.

(23) Li, R.; Liclican, A.; Xu, Y.; Pitts, J.; Niu, C.; Zhang, J.; Kim, C.; Zhao, X.; Soohoo, D.; Babusis, D.; Yue, Q.; Ma, B.; Murray, B. P.; Subramanian, R.; Xie, X.; Zou, J.; Bilello, J. P.; Li, L.; Schultz, B. E.; Sakowicz, R.; Smith, B. J.; Shi, P. Y.; Murakami, E.; Feng, J. Y. Key Metabolic Enzymes Involved in Remdesivir Activation in Human Lung Cells. *Antimicrob. Agents Chemother.* **2021**, *65* (9), No. e0060221.

(24) Xie, X.; Muruato, A. E.; Zhang, X.; Lokugamage, K. G.; Fontes-Garfias, C. R.; Zou, J.; Liu, J.; Ren, P.; Balakrishnan, M.; Cihlar, T.; Tseng, C. K.; Makino, S.; Menachery, V. D.; Bilello, J. P.; Shi, P. Y. A Nanoluciferase SARS-CoV-2 for Rapid Neutralization Testing and Screening of Anti-infective Drugs for COVID-19. *Nat. Commun.* **2020**, *11* (1), 5214.

(25) Do, T. N. D.; Donckers, K.; Vangeel, L.; Chatterjee, A. K.; Gallay, P. A.; Bobardt, M. D.; Bilello, J. P.; Cihlar, T.; De Jonghe, S.; Neyts, J.; Jochmans, D. A Robust SARS-CoV-2 Replication Model in Primary Human Epithelial Cells at the Air Liquid Interface to Assess Antiviral Agents. *Antivir. Res.* **2021**, *192*, No. 105122.

(26) Tao, S.; Zandi, K.; Bassit, L.; Ong, Y. T.; Verma, K.; Liu, P.; Downs-Bowen, J. A.; McBrayer, T.; LeCher, J. C.; Kohler, J. J.; Tedbury, P. R.; Kim, B.; Amblard, F.; Sarafianos, S. G.; Schinazi, R. F. Comparison of Anti-SARS-CoV-2 Activity and Intracellular Metabolism of Remdesivir and its Parent Nucleoside. *Curr. Res. Pharm. Drug Discovery* **2021**, *2*, No. 100045.

(27) Pruijssers, A. J.; George, A. S.; Schäfer, A.; Leist, S. R.; Gralinksi, L. E.; Dinnon, K. H., III; Yount, B. L.; Agostini, M. L.; Stevens, L. J.; Chappell, J. D.; Lu, X.; Hughes, T. M.; Gully, K.; Martinez, D. R.; Brown, A. J.; Graham, R. L.; Perry, J. K.; Du Pont, V.; Pitts, J.; Ma, B.; Babusis, D.; Murakami, E.; Feng, J. Y.; Bilello, J. P.; Porter, D. P.; Cihlar, T.; Baric, R. S.; Denison, M. R.; Sheahan, T. P. Remdesivir Inhibits SARS-CoV-2 in Human Lung Cells and Chimeric SARS-CoV Expressing the SARS-CoV-2 RNA Polymerase in Mice. *Cell Rep.* **2020**, *32*, No. 107940.

(28) Schooley, R. T.; Carlin, A. F.; Beadle, J. R.; Valiaeva, N.; Zhang, X. Q.; Clark, A. E.; McMillan, R. E.; Leibel, S. L.; McVicar, R. N.; Xie, J.; Garretson, A. F.; Smith, V. I.; Murphy, J.; Hostetler, K. Y. Rethinking Remdesivir: Synthesis, Antiviral Activity and Pharmacokinetics of Oral Lipid Prodrugs. *Antimicrob. Agents Chemother.* **2021**, *65*, No. e01155-21.

(29) McGuigan, C.; Harris, S. A.; Daluge, S. M.; Gudmundsson, K. S.; McLean, E. W.; Burnette, T. C.; Marr, H.; Hazen, R.; Condreay, L. D.; Johnson, L.; De Clercq, E.; Balzarini, J. Application of Phosphoramidate Pronucleotide Technology to Abacavir Leads to a Significant Enhancement of Antiviral Potency. *J. Med. Chem.* **2005**, *48* (10), 3504−3515.

(30) Wang, T.; Babusis, D.; Park, Y.; Niu, C.; Kim, C.; Zhao, X.; Lu, B.; Ma, B.; Muench, R. C.; Sperger, D.; Ray, A. S.; Murakami, E. Species Differences in Liver Accumulation and Metabolism of Nucleotide Prodrug Sofosbuvir. *Drug Metab. Pharmacokinet.* **2020**, *35* (3), 334−340.

(31) Liu, A.; Lute, J.; Gu, H.; Wang, B.; Trouba, K. J.; Arnold, M. E.; Aubry, A.-F.; Wang, J. Challenges and Solutions in the Bioanalysis of BMS-986094 and its Metabolites Including a Highly Polar, Active Nucleoside Triphosphate in Plasma and Tissues Using LC-MS/MS. *J. Chromatogr. B. Analyt. Technol. Biomed. Life. Sci.* **2015**, *1000*, 29−40.

(32) Cho, A.; Zhang, L.; Xu, J.; Lee, R.; Butler, T.; Metobo, S.; Aktoudianakis, V.; Lew, W.; Ye, H.; Clarke, M.; Doerffler, E.; Byun, D.; Wang, T.; Babusis, D.; Carey, A. C.; German, P.; Sauer, D.; Zhong, W.; Rossi, S.; Fenaux, M.; McHutchison, J. G.; Perry, J.; Feng, J.; Ray, A. S.; Kim, C. U. Discovery of the First *C*-nucleoside HCV Polymerase Inhibitor (GS-6620) with Demonstrated Antiviral Response in HCV Infected Patients. *J. Med. Chem.* **2014**, *57* (5), 1812−1825.

(33) Good, S. S.; Westover, J.; Jung, K. H.; Zhou, X.-J.; Moussa, A.; La Colla, P.; Collu, G.; Canard, B.; Sommadossi, J.-P. AT-527, a Double Prodrug of a Guanosine Nucleotide Analog, Is a Potent Inhibitor of SARS-CoV-2 *In Vitro* and a Promising Oral Antiviral for Treatment of COVID-19. *Antimicrob. Agents Chemother.* **2021**, *65*, No. e02479-20.

(34) Uckun, F. M.; Waurzyniak, B.; Tibbles, H.; Venkatachalam, T. K.; Erbeck, D. In Vivo Pharmacokinetics and Toxicity Profile of the Anti-HIV Agent Stampidine in Dogs and Feline Immunodeficiency Virus-infected Cats. *Arzneimittelforschung* **2006**, *56* (2A), 176−192.

(35) Karuna, R.; Yokokawa, F.; Wang, K.; Zhang, J.; Xu, H.; Wang, G.; Ding, M.; Chan, W. L.; Abdul Ghafar, N.; Leonardi, A.; Seh, C. C.; Seah, P. G.; Liu, W.; Srinivasa, R. P. S.; Lim, S. P.; Lakshminarayana, S. B.; Growcott, E.; Babu, S.; Fenaux, M.; Zhong, W.; Gu, F.; Shi, P.-Y.; Blasco, F.; Chen, Y.-L. A Cyclic Phosphoramidate Prodrug of 2′-Deoxy-2′-Fluoro-2′-C-Methylguanosine for the Treatment of Dengue Virus Infection. *Antimicrob. Agents Chemother.* **2020**, *64* (12), No. e00654-20.

(36) Cox, R. M.; Wolf, J. D.; Lieber, C. M.; Sourimant, J.; Lin, M. J.; Babusis, D.; DuPont, V.; Chan, J.; Barrett, K. T.; Lye, D.; Kalla, R.; Chun, K.; Mackman, R. L.; Ye, C.; Cihlar, T.; Martinez-Sobrido, L.; Greninger, A. L.; Bilello, J. P.; Plemper, R. K. Oral Prodrug of Remdesivir Parent GS-441524 is Efficacious Against SARS-CoV-2 and a Variant of Concern in Ferrets. *Nat. Commun.* **2021**, *12*, 6415.

(37) Williamson, B. N.; Feldmann, F.; Schwarz, B.; Meade-White, K.; Porter, D. P.; Schulz, J.; van Doremalen, N.; Leighton, I.; Yinda, C. K.; Pérez-Pérez, L.; Okumura, A.; Lovaglio, J.; Hanley, P. W.; Saturday, G.; Bosio, C. M.; Anzick, S.; Barbian, K.; Cihlar, T.; Martens, C.; Scott, D. P.; Munster, V. J.; de Wit, E. Clinical Benefit of Remdesivir in Rhesus Macaques Infected With SARS-CoV-2. *Nature* **2020**, *585*, 273−276.

(38) Humeniuk, R.; Mathias, A.; Cao, H.; Osinusi, A.; Shen, G.; Chng, E.; Ling, J.; Vu, A.; German, P. Safety, Tolerability, and Pharmacokinetics of Remdesivir, An Antiviral for Treatment of COVID-19, in Healthy Subjects. *Clin. Transl. Sci.* **2020**, *13*, 896−906.

(39) Yan, V. C.; Muller, F. L. Advantages of the Parent Nucleoside GS-441524 Over Remdesivir for Covid-19 Treatment. *ACS Med. Chem. Lett.* **2020**, *11* (7), 1361−1366.

(40) Taylor, G. Animal Models of Respiratory Syncytial Virus Infection. *Vaccine* **2017**, *35*, 469−480.